

# Low-loss guided modes in photonic crystal waveguides

Dario Gerace and Lucio Claudio Andreani

Dipartimento di Fisica "A. Volta," Università di Pavia, via Bassi 6, I-27100 Pavia, ITALY

[gerace@fisicavolta.unipv.it](mailto:gerace@fisicavolta.unipv.it)

**Abstract:** We study disorder-induced propagation losses of guided modes in photonic crystal slabs with line-defects. These losses are treated within a theoretical model of size disorder for the etched holes in the otherwise periodic photonic lattice. Comparisons are provided with state-of-the-art experimental data, both in membrane and Silicon-on-Insulator (SOI) structures, in which propagation losses are mainly attributed to fabrication imperfections. The dependence of the losses on the photon group velocity and the useful bandwidth for low-loss propagation are analyzed and discussed for membrane and asymmetric as well as symmetric SOI systems. New designs for further improving device performances are proposed, which employ waveguides with varying channel widths. It is shown that losses in photonic crystal waveguides could be reduced by almost an order of magnitude with respect to latest experimental results. Propagation losses lower than 0.1 dB/mm are predicted for suitably designed structures, by assuming state-of-the-art fabrication accuracy.

© 2005 Optical Society of America

**OCIS codes:** (230.7370) Waveguides; (250.5300) Photonic integrated circuits

---

## References and links

1. E. Yablonovitch, "Inhibited spontaneous emission in solid-state physics and electronics," *Phys. Rev. Lett.* **58**, 2059–2062 (1987).
2. S. John, "Strong localization of photons in certain disordered dielectric superlattices," *Phys. Rev. Lett.* **58**, 2486–2489 (1987).
3. J. D. Joannopoulos, R. D. Meade, and J. N. Winn, *Photonic Crystals: Molding the Flow of Light* (Princeton University Press, Princeton, 1995).
4. K. Sakoda, *Optical Properties of Photonic Crystals* (Springer, Berlin, 2001).
5. S. G. Johnson and J. D. Joannopoulos, *Photonic Crystals: the Road from Theory to Practice* (Kluwer, Dordrecht, 2002).
6. See papers in *IEEE J. Quantum Electron.* **38**, Feature section on *Photonic Crystal Structures and Applications*, edited by T. F. Krauss and T. Baba, pp.724–963 (2002).
7. A. Chutinan and S. Noda, "Waveguides and waveguide bends in two-dimensional photonic crystal slabs," *Phys. Rev. B* **62**, 4488–4492 (2000).
8. S. G. Johnson, P. R. Villeneuve, S. Fan, and J. D. Joannopoulos, "Linear waveguides in photonic crystal slabs," *Phys. Rev. B* **62**, 8212–8222 (2000).
9. M. Qiu, "Band gap effects in asymmetric photonic crystal slabs," *Phys. Rev. B* **66**, 033103 (2002).
10. H. Benisty, D. Labilloy, C. Weisbuch, C. J. .M. Smith, T. F. Krauss, D. Cassagne, A. Béraud, and C. Jouanin, "Radiation losses of waveguide-based two-dimensional photonic crystals: positive role of the substrate," *Appl. Phys. Lett.* **76**, 532 (2000).
11. W. Bogaerts, P. Bienstman, D. Taillaert, R. Baets, and D. De Zutter, "Out-of-plane scattering in photonic crystal slabs," *IEEE Photon. Technol. Lett.* **13**, 565–567 (2001).
12. M. Notomi, A. Shinya, K. Yamada, J. Takahashi, C. Takahashi, and I. Yokohama, "Structural tuning of guiding modes of line-defect waveguides of Silicon-on-Insulator photonic crystal slabs," *IEEE J. Quantum Electron.* **38**, 736–742 (2002).

13. S. J. McNab, N. Moll, and Yu. A. Vlasov, "Ultra-low loss photonic integrated circuit with membrane-type photonic crystal waveguides," *Opt. Express* **11**, 2927–2939 (2003), <http://www.opticsexpress.org/abstract.cfm?URI=OPEX-11-22-2927>.
14. M. Notomi, A. Shinya, S. Mitsugi, E. Kuramochi, and H.-Y. Ryu, "Waveguides, resonators and their coupled elements in photonic crystal slabs," *Opt. Express* **12**, 1551–1561 (2004), <http://www.opticsexpress.org/abstract.cfm?URI=OPEX-12-8-1551>.
15. W. Bogaerts, D. Taillaert, B. Luyssaert, P. Dumon, J. Van Campenhout, P. Bienstman, D. Van Thourhout, and R. Baets, "Basic structures for photonic integrated circuits in Silicon-on-insulator," *Opt. Express* **12**, 1583–1591 (2004), <http://www.opticsexpress.org/abstract.cfm?URI=OPEX-12-8-1583>.
16. Y. Sugimoto, Y. Tanaka, N. Ikeda, Y. Nakamura, K. Asakawa, and K. Inoue, "Low propagation loss of 0.76 dB/mm in GaAs-based single-line-defect two-dimensional photonic crystal slab waveguides up to 1 cm in length," *Opt. Express* **12**, 1090–1096 (2004), <http://www.opticsexpress.org/abstract.cfm?URI=OPEX-12-6-1090>.
17. K. K. Lee, D. R. Lim, H.-C. Luan, A. Agarwal, J. Foresi, and L. C. Kimerling, "Effect of size and roughness on light transmission in a Si/SiO<sub>2</sub> waveguide: experiments and model," *Appl. Phys. Lett.* **77**, 1617–1619 (2000).
18. Yu. A. Vlasov and S. J. McNab, "Losses in single-mode silicon-on-insulator strip waveguides and bends," *Opt. Express* **12**, 1622–1631 (2004), <http://www.opticsexpress.org/abstract.cfm?URI=OPEX-12-8-1622>.
19. W. Bogaerts, P. Bienstman, and R. Baets, "Scattering at sidewall roughness in photonic crystal slabs," *Opt. Lett.* **28**, 689–691 (2003).
20. M. L. Povinelli, S. G. Johnson, E. Lidorikis, J. D. Joannopoulos, and M. Soljačić, "Effect of a photonic band gap on scattering from waveguide disorder," *Appl. Phys. Lett.* **84**, 3639–3641 (2004).
21. Y. Tanaka, T. Asano, Y. Akahane, B.-S. Song, and S. Noda, "Theoretical investigation of a two-dimensional photonic crystal slab with truncated cone air holes," *Appl. Phys. Lett.* **82**, 1661–1663 (2003).
22. Y. Tanaka, T. Asano, R. Hatsuta, and S. Noda, "Analysis of a line-defect waveguide on a Silicon-on-Insulator two-dimensional photonic-crystal slab," *J. Lightwave Technol.* **22**, 2787–2792 (2004).
23. B. Cluzel, D. Gérard, E. Picard, T. Charvolin, V. Calvo, E. Hadji, and F. de Fornel, "Experimental demonstration of Bloch mode parity change in photonic crystal waveguide," *Appl. Phys. Lett.* **85**, 2682–2684 (2004).
24. D. Gerace and L. C. Andreani, "Disorder-induced losses in photonic crystal waveguides with line defects," *Opt. Lett.* **29**, 1897–1899 (2004).
25. L. C. Andreani, D. Gerace, and M. Agio, "Gap maps, diffraction losses and exciton-polaritons in photonic crystal slabs," *Phot. Nanostruct.* **2**, 103–110 (2004).
26. S. Hughes, L. Ramunno, J. F. Young, and J. E. Sipe, "Extrinsic optical scattering loss in photonic crystal waveguides: role of fabrication disorder and photon group velocity," *Phys. Rev. Lett.* **94**, 033903 (2005).
27. K. Yamada, H. Morita, A. Shinya, and M. Notomi, "Improved line-defect structures for photonic-crystal waveguides with high group velocity," *Opt. Commun.* **198**, 395–402 (2001).
28. M. Notomi, K. Yamada, A. Shinya, J. Takahashi, and I. Yokohama, "Extremely large group-velocity dispersion of line-defect waveguides in photonic crystal slabs," *Phys. Rev. Lett.* **87**, 253902 (2001).
29. L. C. Andreani and M. Agio, "Photonic bands and gap maps in a photonic crystal slab," *IEEE J. Quantum Electron.* **38**, 891–898 (2002).
30. T. Ochiai and K. Sakoda, "Nearly free-photon approximation for two-dimensional photonic crystal slabs" *Phys. Rev. B* **64**, 045108 (2001).
31. L. C. Andreani, "Photonic bands and radiation losses in photonic crystal waveguides," *Physica Status Solidi B* **234**, 139 (2002).
32. L. C. Andreani and M. Agio, "Intrinsic diffraction losses in photonic crystal waveguides with line defects," *Appl. Phys. Lett.* **82**, 2011–2013 (2003).
33. M. Skorobogatiy, G. Bégin, and A. Talneau, "Statistical analysis of geometrical imperfections from the images of 2D photonic crystals," *Opt. Express* **13**, 2487–2502 (2005), <http://www.opticsexpress.org/abstract.cfm?URI=OPEX-13-7-2487>.
34. M. Galli, D. Bajoni, M. Patrini, G. Guizzetti, D. Gerace, L. C. Andreani, M. Belotti, and Y. Chen, "Single-mode versus multi-mode behavior in Silicon photonic crystal waveguides measured by attenuated total reflectance," submitted to *Phys. Rev. B*.
35. D. Marcuse, "Mode conversion caused by surface imperfections of a dielectric slab waveguide," *Bell. Syst. Tech. J.* **48**, 3187 (1969).
36. F. P. Payne and J. P. R. Lacey, "A theoretical analysis of scattering loss from planar optical waveguides," *Opt. Quant. Electron.* **26**, 977–986 (1994).
37. F. Grillot, L. Vivien, S. Laval, D. Pascal, and E. Cassan, "Size influence on the propagation loss induced by side-wall roughness in ultra-small SOI waveguides," *IEEE Photon. Technol. Lett.* **16**, 1661–1663 (2004).

## 1. Introduction

Photonic crystals (PhC) exploit the periodicity of the refractive index as a mean to artificially manipulate the confinement and propagation characteristics of light in three dimensions [1, 2, 3]. Owing to the difficulties in fabricating fully three-dimensional periodic systems with controlled defects at optical wavelengths, two-dimensional photonic crystals embedded in planar waveguides are emerging as important candidates for prospective applications to integrated optics [4, 5, 6]. In such systems, also called PhC slabs, the in-plane confinement of light provided by the spatial periodicity of an etched dielectric material is added to the usual dielectric guiding mechanism along the vertical direction.

In recent years, it has become of crucial importance to understand the out-of-plane scattering of light, leading to attenuation and losses in photonic integrated waveguides and resonators realized in PhC slabs. As it is known, these systems support both truly- and quasi-guided photonic eigenmodes, the latter falling above the light line of the cladding material (or materials, if the waveguide is asymmetric) surrounding the guiding dielectric layer [7, 8, 9]. Whilst quasi-guided modes suffer from intrinsic radiative losses out of the slab plane due to the periodic pattern [10, 11], truly guided modes should be lossless in an ideal PhC structure without imperfections. For this reason such modes have attracted great attention in view of exploiting PhC waveguides as optical interconnects in all-optical chips, thus avoiding significant signal loss. In real systems, truly guided modes are subject to out-of-plane scattering losses due to fabrication imperfections and roughness, and research has been focusing on the problem of reducing such unwanted losses by means of an improved fabrication accuracy. Though excellent results have been recently obtained both in Silicon [12, 13, 14, 15] and GaAs-based structures [16], it is still true that propagation losses in PhC systems are too large as compared to competing strip waveguides [17, 18]. From a theoretical point of view, little work has been done concerning the role of fabrication imperfections on out-of-plane losses in PhC slabs, up to date. The main works concern the role of side-wall roughness [19, 20] and the scattering of TE-like modes into TM-like ones induced by vertical asymmetry of the structures (such as truncated cone-shaped etched holes, or the presence of two different cladding materials) [21, 22]. A Bloch mode parity change due to asymmetries in the waveguide channel has been recently confirmed experimentally [23], pointing out the importance of realizing single-mode propagation in PhC waveguides. Recently, we have developed a fast and accurate tool to study the role of disorder on the extrinsic losses, and we have performed systematic studies on the dependence of such losses as a function of various structure parameters [24, 25]. Furthermore, a study concerning the role of disorder on the scattering losses of defect modes in PhC waveguides has been recently published by Hughes et al. [26], based on a Green's function tensor approach. The latter work confirms some of the results reported in Ref. [24], regarding in particular the highly dispersive nature of the losses and the crucial role played by the group velocity ( $v_g$ ) of the defect mode, by using a more fundamental theoretical approach. The importance of the group velocity for low-loss propagation was previously stressed in Refs. [27, 28].

The idea of the present work is to perform a more quantitative comparison with available experimental results, thus proving the reliability of our theoretical method and our model of disorder. State-of-the-art experimental results taken from the literature and related to structures in both membrane and Silicon-on-Insulator (SOI) configurations are addressed for such comparisons. We then propose new structure designs, in which the combined use of current fabrication accuracy and of a suitably designed guided mode dispersion should allow to realize the lowest possible values for propagation losses below the light line in linear waveguides with varying channel widths. In our theoretical analysis we consider PhC slabs in membrane and in asymmetric as well as symmetric SOI vertical guiding structures. We point out the importance of using PhC waveguides with single-mode behavior, and make a comparison with losses in

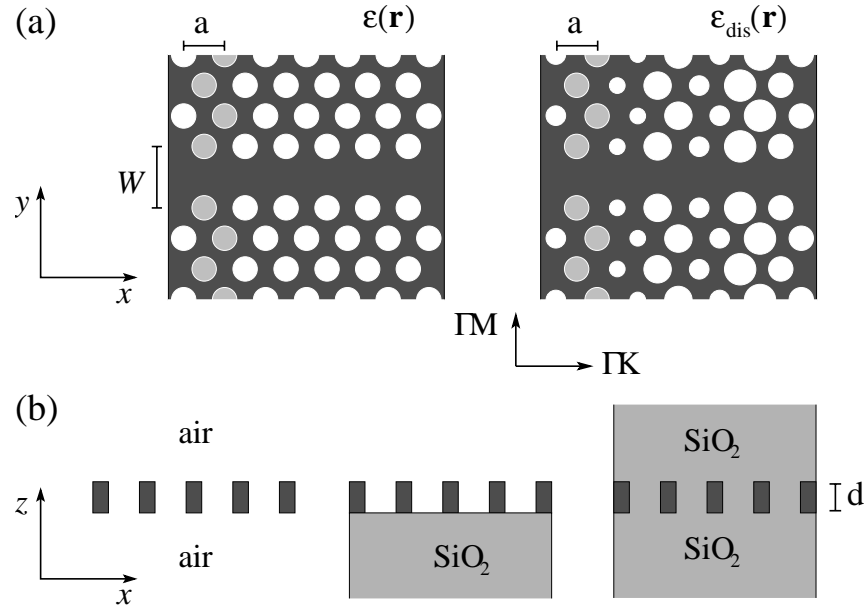


Fig. 1. Schematic pictures of systems under study in the present work. (a) Line-defect along the  $\Gamma$ -K direction for the unperturbed and disordered triangular lattices in the  $(x,y)$  plane; the effect of a random variation of holes radii has been exaggerated. Light gray holes represent the fundamental cell to be repeated with supercell periodicity in a square lattice. The main symmetry directions of the triangular lattice,  $\Gamma$ -K and  $\Gamma$ -M, are also defined. (b) Vertical guiding structures considered in this work: (from left to right) the air-clad, the asymmetric  $\text{SiO}_2$ -clad, and the symmetric  $\text{SiO}_2$ -clad photonic crystal waveguides.

conventional strip waveguides under the same conditions.

The paper is organized as follows. In Section 2, the theoretical model is briefly introduced and discussed; in Section 3, recently published experimental results are analyzed in order to get reliable disorder parameters, consistent with current micro-fabrication technology. In Section 4, new structures are studied and new design concepts are proposed. Finally, the conclusions of the work are discussed.

## 2. A theoretical model of disorder

As it is well established, disorder-induced scattering of light is the main source of propagation losses for guided modes in PhC waveguides. We accounted for this loss mechanism within a simplified theoretical model of random size fluctuations in the etched holes (see also Refs. [24] and [25] for details).

Briefly, the theoretical approach adopted here is based on a recently developed guided-mode expansion method [29], in which the field is expanded on the basis of the guided modes of an effective homogeneous waveguide with averaged dielectric constant in the plane. This method allows to obtain the photonic mode dispersion both above and below the light line. Dielectric perturbations couple guided or quasi-guided modes to the radiative modes of the same “effective” waveguide used to calculate the set of modes for the expansion. This coupling is taken into account by a photonic version of time-dependent perturbation theory [30, 31]. The latter yields an imaginary part of mode frequencies,  $\text{Im}(\omega)$ , which is related to the mode finite life-

time due to the coupling to radiative modes. A systematic study of intrinsic out-of-plane losses of quasi-guided modes, induced by the in-plane dielectric periodicity in PhC slabs has been already reported in Ref. [32]. For truly-guided modes, disorder is taken into account only in the perturbative calculation of losses, where the unperturbed modes (i.e. the ones calculated for the system without disorder) are coupled to the radiative modes owing to the large supercell introduced to describe the hole size fluctuations [24]. These fluctuations are described by a random distribution of hole radii, with Gaussian probability, around an average value  $r$ . The root mean square (r.m.s.) deviation of the radius,  $\Delta r$ , is taken as the unique disorder parameter. The coupling yields an imaginary part of mode frequencies also when the unperturbed mode falls below the light line. Propagation losses of guided modes are defined as  $\alpha_{\text{loss}} = 2\text{Im}(k) = 2\text{Im}(\omega)/v_g$ , where the loss coefficient  $\alpha_{\text{loss}}$  is usually measured in dB/mm and is related to the attenuation of light intensity.

The choice of the basis for the expansion makes the method particularly suited to study systems with a strong refractive index contrast between the core layer and the claddings. For what concerns suspended dielectric membranes or air/dielectric/oxide structures, photonic eigenmodes obtained by the present approach can be considered reliable and accurate within a few percent error. In the present work we restrict ourselves to considering high index contrast structures.

We consider a triangular lattice of holes with lattice constant  $a$ , in which a line-defect consisting of a missing row of holes along the  $\Gamma$ -K direction is introduced (see Fig. 1 for a schematic picture of the structure and a definition of the symmetry directions of the triangular lattice). The system is realized on a PhC slab of thickness  $d$  patterned in a high-index material. A waveguide with channel width  $W = W_0 = \sqrt{3}a$  is called a W1.0 waveguide. Increased- or reduced-width waveguides can be defined by modifying the channel width as  $W = X \cdot W_0$ , where  $X$  is a real multiplication factor. A schematic picture of the in-plane supercell employed in the calculations of disorder-induced losses is shown in Fig. 1(a), where the r.m.s. deviation has been exaggerated for clarity. The disordered lattice is constructed after supercell repetition of the fundamental cell (shaded holes in figure) along the  $\Gamma$ -K direction. The dielectric perturbation leading to extrinsic losses is given by  $\Delta\epsilon(\mathbf{r}) = \epsilon_{\text{dis}}(\mathbf{r}) - \epsilon(\mathbf{r})$ , where  $\epsilon(\mathbf{r})$  is the spatially-dependent dielectric function of the ideal lattice and  $\epsilon_{\text{dis}}(\mathbf{r})$  is the dielectric function of the disordered lattice. Only size variation along the  $\Gamma$ -K direction is relevant and is taken into account.

We point out that our model takes into account only size disorder, described by a r.m.s. deviation  $\Delta r$  of the radius. In the sample fabrication procedure, this roughness parameter depends on the mask transfer and etching process, as it is related to the resolution of the polymeric resist upon exposure and development, and is usually of the order of a few nanometers. We do not consider position disorder (i.e., variation of the hole-to-hole distance), which is determined instead by the alignment of the electron-beam lithography process and can be made smaller than size disorder [28]. While a more complete model of disorder should take into account both effects as measured in real samples [33], in the present work we focus on the size-disorder, single-parameter model. While the exact numbers for the losses may depend on the specific properties of the hole sidewalls, the trends and the design rules following from the present model are believed to have more general validity.

In Fig. 1(b) the vertical guiding structures considered in this work are schematically shown. In particular, we consider air-clad PhC waveguides, SOI or asymmetric SiO<sub>2</sub>-clad structures in which the Silicon layer is grown on top of an oxide cladding, and symmetric SiO<sub>2</sub>-clad PhC waveguides where an upper SiO<sub>2</sub> cladding is deposited after patterning of the core. The dielectric constants used throughout this work are  $\epsilon_{\text{dielectric}} = 12.11$  and  $\epsilon_{\text{oxide}} = 2.08$  for Silicon and SiO<sub>2</sub> materials, respectively. These values are appropriate for such materials when considering the wavelength range around 1.55 μm. In the present work, a supercell of size  $8W_0 + W$  is used

in the direction perpendicular to the line defect for the calculations of photonic mode dispersion; disorder-induced losses are calculated by using a supercell of size  $49a$  along the  $\Gamma$ -K direction in the perturbative treatment, and an average over six different Gaussian distributions of hole radii with the same r.m.s. deviation is performed to get final results. The number of plane waves and guided modes taken in the basis set has been chosen, according to convergence tests, in order to get an accuracy of the order of a percent for the losses.

Considering the geometry of Fig. 1, and taking the origin of the  $z$  axis to be at the middle of the slab, specular reflection with respect to the  $(x,y)$  plane is a symmetry operation for air-clad or symmetric  $\text{SiO}_2$ -clad PhC waveguides, which we denote by  $\hat{\sigma}_{xy}$ . When dealing with symmetric PhC waveguides, we consider only modes with  $\sigma_{xy} = +1$  (sometimes called TE-like modes) for which the triangular lattice has a band gap in all directions. For asymmetric structures, like SOI, modes with both parities must be included in the basis set. Furthermore, for any kind of vertical structure, defect modes can be classified according to reflection symmetry with respect to the vertical plane bisecting the waveguide channel, denoted as  $\hat{\sigma}_{kz} \equiv \hat{\sigma}_{xz}$  operation: odd (even) modes are classified as  $\sigma_{kz} = -1$  ( $\sigma_{kz} = +1$ ).

As a final comment, it should be noted that the Green's functions approach of Ref. [26] is, at least in principle, more accurate than ours. In particular, it takes into account backscattering onto the counter-propagating mode, which is not included in the present treatment. On the other hand, the perturbative approach adopted here is faster and computationally more efficient, whilst the Green's function approach needs a calculation of the exact quantities for the unperturbed system, i.e. without disorder, via, e.g., FDTD simulations [26]. In fact, the present method allows a thorough systematic analysis of systems with varying structural parameters, and therefore it is believed to be more suited to design purposes.

### 3. Determination of disorder parameters

We proceed in the following way to the analysis of state-of-the-art experimental data. Our model of disorder is first applied to the air-clad W1.0 PhC waveguide, and then to the SOI W0.7 system. Taking Ref. [14] as a guide, we recover reasonable disorder parameters  $\Delta r$  by reproducing the experimentally measured values of propagation losses.

#### 3.1. Losses in Silicon membranes

A typical structure employed in the experiments in order to measure very low propagation losses, namely the air-clad W1.0 PhC waveguide, is considered here. We assume a lattice constant  $a = 400$  nm and a Silicon core thickness  $d = 220$  nm ( $d/a = 0.55$ ). The average hole radius is fixed at  $r/a = 0.275$ . Experimental data reported in Ref. [14] are briefly analyzed. We calculate the losses only for the  $\sigma_{kz} = -1$  mode. Such modes are usually considered the most interesting for applications, as they have an even spatial profile of the field intensity (no nodes at the middle of the waveguide channel). In an ideal system without imperfections, modes with different  $\hat{\sigma}_{kz}$  should be completely uncoupled. In realistic structures, asymmetries between the two sides of the waveguide channel are responsible for parity mixing between  $\sigma_{kz} = +1$  and  $\sigma_{kz} = -1$  modes, as it was recently demonstrated [23]. For such reason only the true single-mode propagation region should be useful for applications.

In Fig. 2 the photonic mode dispersion is represented in dimensionless units,  $a/\lambda$  for the frequency and  $ka/\pi$  for the wave vector, on both axes. For a lattice constant  $a = 400$  nm the  $\sigma_{kz} = -1$  defect mode dispersion is centered around  $\lambda = 1.5$   $\mu\text{m}$  ( $a/\lambda \simeq 0.267$ ) below the light line. The shaded region represents the continuum of TE-like slab modes of the triangular lattice folded in the line-defect Brillouin zone. On the right hand side, propagation losses are plotted only for what concerns the single-mode frequency region of the  $\sigma_{kz} = -1$  defect mode, on a logarithmic scale on the abscissas. The different curves correspond to different values

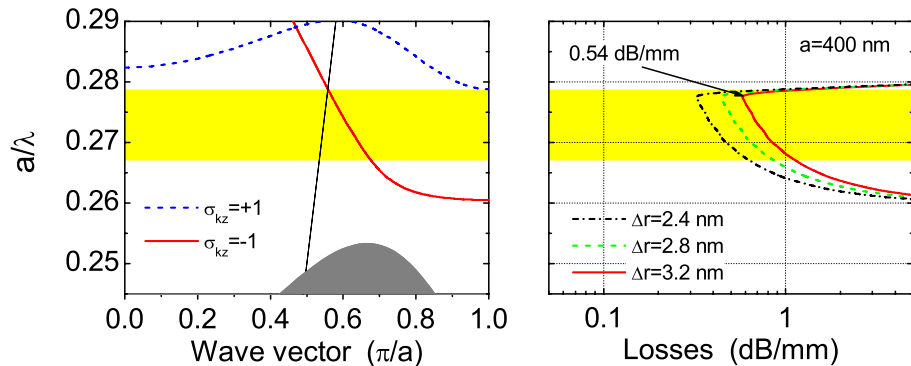


Fig. 2. Calculated photonic dispersion of TE-like modes in a W1.0 waveguide realized in a  $d = 220$  nm thick Silicon membrane patterned with a triangular lattice of air holes ( $r/a = 0.275$ , lattice constant  $a = 400$  nm), and out-of-plane propagation losses corresponding to the  $\sigma_{kz} = -1$  defect mode for different values of the disorder parameter. The low-loss single-mode frequency window is highlighted.

of the disorder parameter. According to these calculations, experimental values of  $0.5 - 0.6$  dB/mm are reproduced with a disorder parameter  $\Delta r/a = 0.008$ , which means that the average uncertainty on the hole radius should be of the order of  $\Delta r = 3.2$  nm. As it can be noticed from Fig. 2, the actual low-loss frequency range for the mode considered here (which is highlighted in the figure) is much narrower than the whole single-mode propagation region. This is due to the strong dependence of propagation losses on the group velocity, which implies that the low group velocity region may be detrimental for future all-optical integration [26, 27]. By defining the low-loss spectral region as the frequency range for which propagation losses are lower than twice the minimum calculated value (this criterion will be employed also in the following figures), only the region between  $a/\lambda \simeq 0.267$  ( $\lambda \sim 1.5$   $\mu\text{m}$  for  $a = 400$  nm) and  $a/\lambda \simeq 0.279$  ( $\lambda \sim 1.43$   $\mu\text{m}$ ) is highlighted, corresponding to a low-loss bandwidth of  $\sim 70$  nm.

### 3.2. Losses in SOI waveguides

In order to put our theoretical model on firm basis, we also reproduced experimentally reported values for propagation losses in asymmetric  $\text{SiO}_2$ -clad PhC waveguides. The difference with respect to the symmetric air-clad structure is that the Si layer is grown on top of a semi-infinite  $\text{SiO}_2$  cladding, as schematically depicted in the central picture of Fig. 1(b). In such kind of structures, it is well established from the literature that the low-loss propagation region below the light line is sensitively reduced by the presence of the  $\text{SiO}_2$  light line. The problem of having a defect mode dispersion with a high group velocity below the light line is solved by using reduced-width PhC waveguides [12, 27]. Thus, a typical structure employed in the experiments is a W0.7 PhC waveguide, in which the channel width is defined as  $W = 0.7 \cdot \sqrt{3}a$ .

We consider here a PhC slab with the same structure parameters as the air-clad PhC waveguide of Fig. 2, i.e. a Silicon core layer of thickness  $d = 220$  nm, with  $r/a = 0.275$  and  $a = 400$  nm. The defect mode dispersion and the corresponding losses at different r.m.s. deviations are shown for the W0.7 SOI waveguide in Fig. 3. A disorder parameter  $\Delta r = 2.2$  nm is found to give a good quantitative agreement with the experimental value (1.5 dB/mm) reported for an analogous SOI structure [14]. The lower  $\Delta r$  value with respect to membrane samples could be considered a theoretical confirmation of the partial smoothing and reduction of roughness in SOI structures with respect to membrane ones. It can be seen from the dispersion of

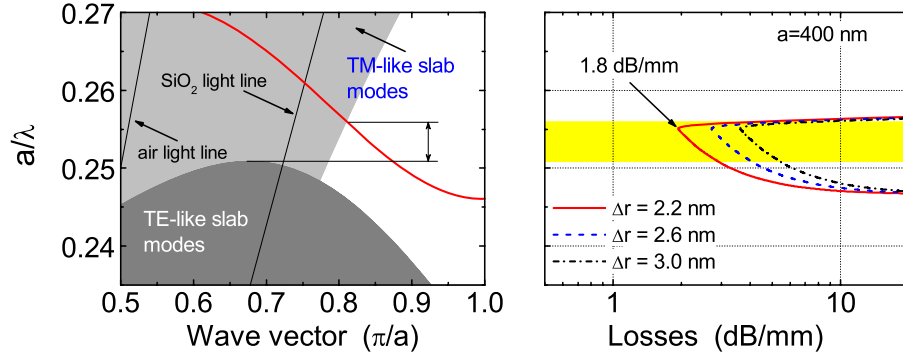


Fig. 3. Calculated photonic mode dispersion of a W0.7 PhC waveguide realized in a  $d = 220$  nm thick SOI system patterned with a triangular lattice of air holes ( $r/a = 0.275$ , lattice constant  $a = 400$  nm), and out-of-plane propagation losses corresponding to the  $\sigma_{k_z} = -1$  defect mode. The low-loss frequency range is highlighted.

Fig. 3 that the propagation region below the light line is also reduced by the presence of the projected TM-like slab modes, which form a continuum of states and allow defining a *TM-slab light line*, as also discussed in Refs. [21, 22]. This is due to the vertical asymmetry of the structure, which implies that  $\hat{\sigma}_{xy}$  is no more a symmetry operation for the system. Such TM-slab light line may be very detrimental for achieving a large propagation bandwidth below the light line, thus considerably limiting the functionality of real devices fabricated on asymmetric SiO<sub>2</sub>-clad PhC waveguides. The low-loss frequency window highlighted in figure has a wavelength bandwidth of  $\sim 30$  nm, i.e. from  $a/\lambda \sim 0.251$  to  $a/\lambda \sim 0.256$  in dimensionless units, and it is again limited by the strong dispersion as a function of the group velocity of the defect mode. On the low energy side, the highlighted region has been limited to the TE-slab modes band edge (dark gray area in figure). Indeed, propagation losses due to scattering between the guided mode and the extended slab modes is not supposed to occur in straight line-defect waveguides, because no overlap exists between such modes in the Brillouin zone. Yet, in realistic photonic integrated circuits the presence of point defects or bends could induce such unwanted scattering mechanism, which thus would limit the effective low-loss propagation bandwidth. For this reason, only the propagation region above the photonic band edge of TE-like slab modes is considered [22], also in the following figures.

As a final remark to this Section, it should be noted that our results usually show minimum values for propagation losses correspondingly to the frequency at which the defect mode dispersion crosses the light line (air light line in the case of PhC membranes and TM-slab light line in the case of SOI structures). We point out that inclusion of the backscattering term in the calculations may lead to a smoothing of the loss curves [26]. In particular, such term is important in the low group velocity region, where the backscattering contribution ( $\propto 1/v_g^2$ ) is not negligible as compared to the main contribution ( $\propto 1/v_g$ ) to propagation losses. In any case, the overall physical behavior and the design considerations discussed in the following should not be affected by this phenomenon.

#### 4. Design concepts for large-bandwidth and low-loss guided modes

In order to exploit state-of-the-art fabrication accuracy, estimated in the previous Section by fitting experimental values for disorder-induced losses, PhC waveguides in different slab geometries are analyzed in this Section, in order to find new designs for large-bandwidth and low-loss

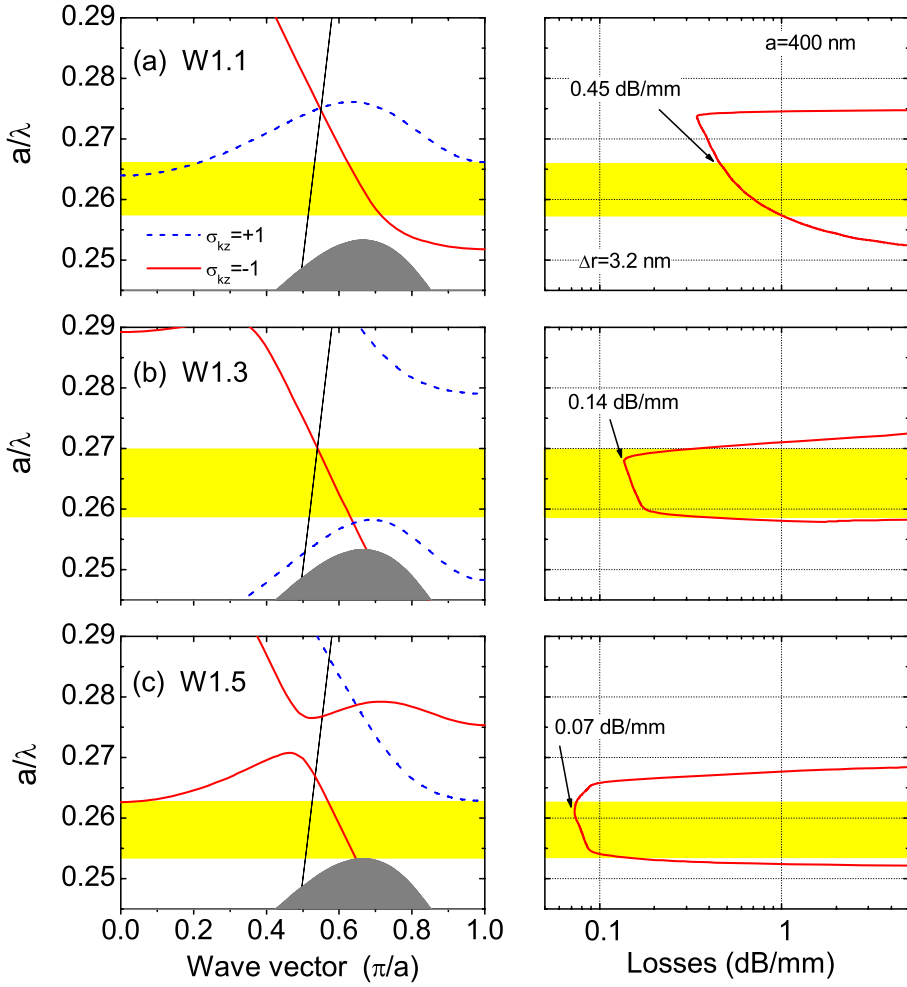


Fig. 4. Calculated photonic dispersion of TE-like modes in air-clad PhC waveguides of channel widths (a)  $W = 1.1 \cdot \sqrt{3}a$ , (b)  $W = 1.3 \cdot \sqrt{3}a$  and (c)  $W = 1.5 \cdot \sqrt{3}a$ , realized in a  $d = 220$  nm thick Silicon membrane patterned with a triangular lattice of air holes ( $r/a = 0.275$ , lattice constant  $a = 400$  nm), and corresponding out-of-plane propagation losses related to the  $\sigma_{kz} = -1$  defect mode below the light line. Highlighted regions correspond to the single-mode low-loss propagation range.

propagation conditions of guided modes below the light line. Realistic PhC waveguides etched in air-clad as well as asymmetric and symmetric SiO<sub>2</sub>-clad waveguides are considered, respectively. The latter structure implies that the Si core be filled and covered with SiO<sub>2</sub> in order to symmetrize the original SOI structure, as shown in the right panel of Fig. 1(b).

#### 4.1. Increased-width waveguides in air-clad PhC slabs

Systematic studies on propagation losses below the light line as a function of various structure parameters, such as hole radius and core thickness, have been reported for membrane-type PhC waveguides [24]. One of the possible strategies to reduce propagation losses in such systems is to increase the waveguide channel width, as previously discussed in Ref. [25]. In the present

work, we extend previously reported considerations to realistic structures with estimated fabrication accuracy, and calculate very low values for propagation losses for increased-width waveguides.

In Fig. 4 the photonic mode dispersion and the corresponding propagation losses are shown for (a) W1.1, (b) W1.3 and (c) W1.5 air-clad PhC waveguides, respectively. The parameters assumed for the structures are the same as in the calculations shown in Fig. 2 for the W1.0 waveguide. As it can be seen from Fig. 4(c), a wide single-mode propagation frequency range is still present below the light line for the  $\sigma_{kz} = -1$  defect mode in the W1.5 waveguide, and for a lattice constant  $a = 400$  nm it is centered around  $\lambda = 1.53 \mu\text{m}$ . *The interesting point is that the effective bandwidth with low-loss propagation is not much different from the W1.0 waveguide.* By using the same criterion as in Fig. 2, the low-loss guided mode region is defined from  $a/\lambda \simeq 0.253$  ( $\lambda \sim 1.58 \mu\text{m}$  for  $a = 400$  nm) to  $a/\lambda \simeq 0.263$  ( $\lambda \sim 1.52 \mu\text{m}$ ) in Fig. 4(c), which is about 60 nm bandwidth. The single-mode dispersion of the  $\sigma_{kz} = -1$  guided mode below the light line has been recently demonstrated by an attenuated total reflectance excitation of the evanescent modes in a single membrane-type W1.5 PhC waveguide [34]. An even larger bandwidth ( $\sim 65$  nm) is predicted for the W1.3 waveguide, as shown in Fig. 4(b), at the expense of slightly higher losses. Propagation losses of the  $\sigma_{kz} = -1$  defect mode decrease on increasing the channel width with respect to the typical W1.0 waveguide, when the same disorder parameter is assumed in the calculations. A clear trend can be seen in the right panels of Fig. 4, in which the minimum loss values are sensitively lowered on going from the W1.1 to the W1.5 structure. It can be also noted that in the W1.3 and W1.5 cases propagation losses are less dispersive than in the W1.0 waveguide, *because the whole single-mode region available is fully related to a high group velocity dispersion of the guided mode.* For the W1.5 air-clad PhC waveguide, the minimum loss value calculated here (predicted by assuming a r.m.s. deviation  $\Delta r = 3.2$  nm) is well below 0.1 dB/mm. Waveguides with channel width  $W > 1.5W_0$  are not considered here as they have no single-mode propagation region below the light line, as we have concluded from a systematic study of the dispersion relations (not shown). Multi-mode waveguides are expected to have larger losses, especially in the presence of localized scattering structures like bends and cavities. It appears that the W1.5 waveguide is the optimal structure in the air-clad system which yields a large-bandwidth, low-loss propagation region.

When such small values for propagation losses below the light line are aimed at, the problem of vertical tapering in the etched holes has to be considered. Non-verticity of the hole sidewalls gives rise to additional losses in the region of TM-like slab modes. For the case of the W1.0 waveguide, it has been calculated that tapering angles of  $1^\circ$  produce losses of the order of 0.5 dB/mm [21]. On increasing the channel width, these losses are expected to decrease with the same trend shown in Fig. 4. Thus, the design concepts discussed in this Section remain valid also in the presence of tapered holes.

It is interesting to compare the propagation losses in linear PhC waveguides with those of Silicon strip waveguides, which are the competing system for integrated optical interconnects. The comparison should be made for structures with the optimal parameters that yield single-mode propagation and low loss. From the experimental side, a recent paper [18] reports losses of the order of 0.36 dB/mm in SOI-based Silicon wires with  $450 \text{ nm} \times 220 \text{ nm}$  cross section. From the theoretical point of view, the losses in strip waveguides are usually calculated within a statistical model containing two parameters, namely a r.m.s. roughness parameter  $\sigma$  and a correlation length  $L_c$  of the size fluctuations [17, 35, 36, 37]. In the present model of size disorder for PhC waveguides, the analog of  $L_c$  is the hole circumference  $2\pi r$ , which is  $\sim 690$  nm with the parameters of Fig. 4. If we compare with the calculated losses of single-mode Si/SiO<sub>2</sub> strip waveguides with  $\sigma = 3.2$  nm and  $L_c = 690$  nm, values of the order of 0.2-0.3 dB/mm are found [17, 37]. These comparisons suggest that propagation losses of W1.5 PhC

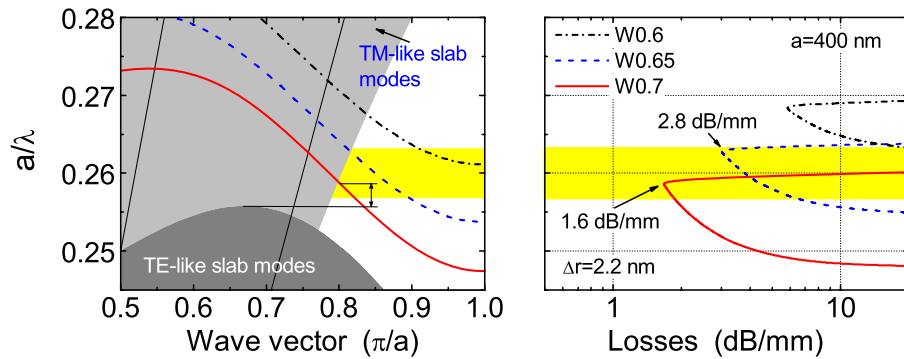


Fig. 5. Calculated photonic dispersion and propagation losses of guided modes in reduced-width PhC waveguides realized in a SOI structure, as schematically represented in Fig. 1(b) (picture in the middle), for different widths of the waveguide channel. Parameters are:  $d/a = 0.5$ ,  $r/a = 0.26$ ,  $a = 400$  nm. The highlighted spectral region on the right refers to the  $\sigma_{k_z} = -1$  defect mode with the largest low-loss propagation bandwidth (W0.65 waveguide).

waveguides can be lower than those of existing Silicon strip waveguides. A more complete analysis of the whole problem should consider the role of the correlation length  $L_c$  within a micro-roughness model for the hole sidewalls in PhC waveguides. Such an analysis is presently under study and will be reported elsewhere.

#### 4.2. Reduced-width waveguides in asymmetric $\text{SiO}_2$ -clad PhC slabs

In SOI-based PhC slabs, the presence of the lower oxide cladding greatly enhances the mechanical stability of the whole structure, in a system that exploits mature nanofabrication technology and know-how coming from current microelectronics industry. It would be desirable, in view of achieving photonics integration based on PhC slab systems, an all-optical chip made upon a SOI platform other than a suspended Silicon structure. For such reasons, much effort has been devoted to the improvement of experimental results discussed in Sec. 3.2. As it has been pointed out, one of the main physical limitations of SOI systems is the existence of the TM-slab light line, which considerably reduces the available bandwidth for low-loss propagation.

In order to overcome some of these limiting issues, besides the use of reduced-width waveguides to increase the high group velocity region below the light line [27], some design concepts for the optimization of the SOI-based structures have been suggested [22]. In particular, it has been claimed that a thinner slab thickness and a reduced air fraction should yield larger bandwidth of the propagating defect mode.

According to the suggestions given in Ref. [22], we show in Fig. 5 the defect mode dispersion and the related propagation losses for reduced-width PhC waveguides, in which the structure parameters are slightly modified with respect to Fig. 3. The minimum value for the losses is found for the W0.7 waveguide and it is slightly lower than that reported in Fig. 3, at fixed r.m.s. deviation  $\Delta r = 2.2$  nm. Following the same criterion employed in Fig. 3, only the propagation region above the photonic band edge of TE-like slab modes is considered here. As a consequence, the optimized structure should be the W0.65, in which the low-loss propagation bandwidth is  $\sim 35$  nm, i.e. almost twice the propagation bandwidth of the W0.7 waveguide that is also indicated in figure. Moreover, reasonably low propagation losses are found for the W0.65 structure, even if they are slightly larger than the losses of the W0.7 waveguide.

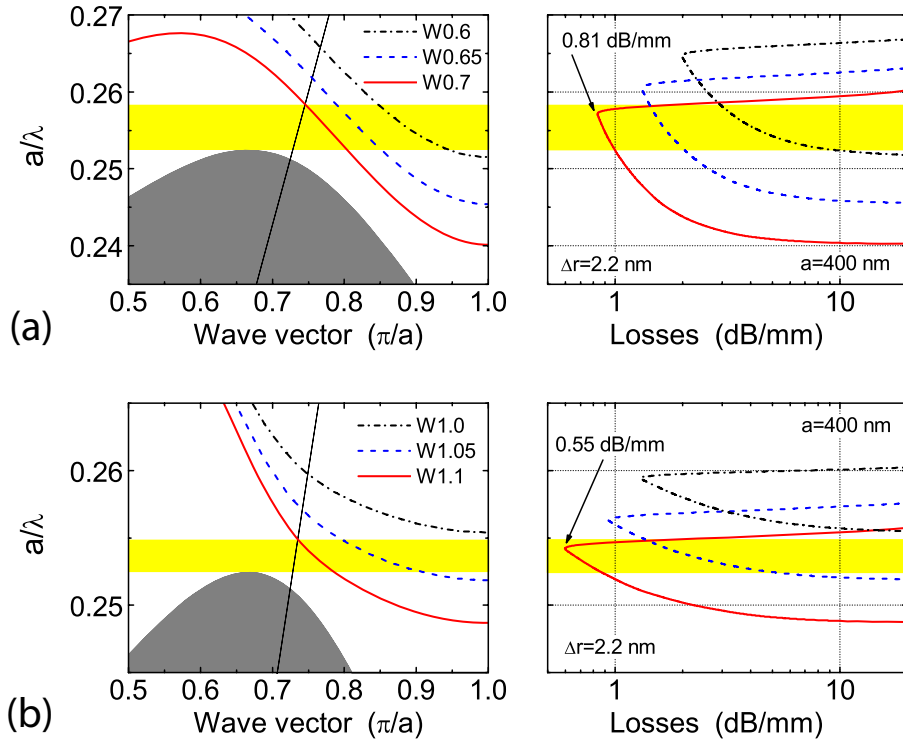


Fig. 6. Calculated photonic dispersion and related propagation losses of TE-like modes in PhC waveguides realized in a Silicon core sandwiched between  $\text{SiO}_2$  claddings and with  $\text{SiO}_2$  in the patterned holes, as schematically represented in Fig. 1(b) (picture on the right). Parameters are:  $d/a = 0.5$ ,  $r/a = 0.26$ ,  $a = 400 \text{ nm}$ . (a) Reduced-width waveguides, and (b) increased width waveguides. The spectral regions of the  $\sigma_{kz} = -1$  defect mode with the lowest propagation losses (W0.7 and W1.1 waveguides, respectively) in the single-mode frequency window are also highlighted.

These results substantially confirm some of the conclusions reported in Ref. [22] about the optimal structure parameters for SOI-based PhC waveguides. Furthermore, the calculations of disorder-induced losses presented here indicate the conditions for an optimal compromise between reduced propagation losses and useful low-loss bandwidth.

#### 4.3. Waveguides in symmetric $\text{SiO}_2$ -clad PhC slabs

In order to increase the low-loss propagation bandwidth in SOI-based systems, a good strategy could be to symmetrize the structure by filling the patterned Silicon core layer between  $\text{SiO}_2$  claddings. In order to compare this structure to the corresponding SOI PhC waveguide of Fig. 5, the calculated photonic dispersion and propagation losses for the  $\sigma_{kz} = -1$  defect mode are shown in Fig. 6 for a symmetric  $\text{SiO}_2$ -clad PhC waveguide. Both reduced- and increased-width waveguides have been systematically analyzed, and the choice of structure parameters for the calculations shown here follows from a detailed study aimed at optimizing both propagation bandwidth and losses.

Results are shown in Figs. 6(a) and (b) for optimized reduced- and increased-width waveguides, respectively. The r.m.s. deviation for disorder calculations is assumed to be the same as the one for the SOI structure. It should be noted that in real structures such value could

be even smaller, owing to the oxidation smoothing within the patterned holes. For a lattice constant  $a = 400$  nm, the useful propagation region of the defect mode is centered around  $1.55 \mu\text{m}$ . The symmetry operation  $\hat{\sigma}_{xy}$  is now allowed, and we consider only TE-like modes ( $\sigma_{xy} = +1$ ). As it can be seen by comparing Figs. 5 and 6(a), the low-loss propagation region for the W0.7 structure is slightly increased ( $\sim 40$  nm), owing to the existence of a complete band gap for TE-like modes (analogous to the air-clad structure), for which the TM-slab light line is not present. Results for propagation losses, shown on the right hand side of Fig. 6(a), show that they could be reduced by more than a factor of two with respect to the corresponding SOI structure, while having almost twice the propagation bandwidth of the W0.7 SOI waveguide. In Fig. 6(b), results are shown for increased-width waveguides in symmetric SiO<sub>2</sub>-clad structures. Although in this case the useful low-loss bandwidth is considerably smaller than in the optimized reduced-width waveguide, very low values for the propagation losses could be achieved in W1.1 waveguides, with an available bandwidth of  $\sim 20$  nm. Such predicted values are comparable to measured values of state-of-the-art propagation losses in membrane-type W1.0 waveguides (see Fig. 2).

## 5. Conclusions

In summary, it has been shown that very low propagation losses may be achieved in Silicon-based photonic crystal waveguides by the combined use of highly developed fabrication technology and properly designed guided mode dispersion.

By using disorder parameters determined from state-of-the-art experimental results, calculations of photonic mode dispersion and disorder-induced propagation losses of guided modes have been carried out for both membrane-type and SOI-based systems. As a general consideration in designing photonic crystal waveguides with large propagation bandwidth in the low-loss frequency region below the light line, care must be taken in ensuring single-mode behavior and high group velocity of the corresponding guided mode. Indeed, propagation losses may increase by orders of magnitude in the low group velocity region of the guided mode dispersion. New design concepts have been proposed in order to overcome such drawbacks in photonic crystal waveguides. For membrane-type structures, it has been shown that increasing the waveguide channel width to  $W = 1.5W_0$  should allow achieving a large propagation bandwidth with predicted losses well below 0.1 dB/mm. For what concerns SOI-based waveguides, symmetrization of the vertical guiding structure, so-called symmetric SiO<sub>2</sub>-clad structures, should give larger propagation bandwidths and lower losses than in similar asymmetric structures.

Our calculated losses for optimized PhC waveguides are lower than in state-of-the-art Silicon strip waveguides. The lower losses of PhC waveguides follow from two main reasons: (i) the tailoring of dispersion relations of line-defect modes, which enables achieving single-mode propagation for relatively large channel widths and (ii) the possibility of fabricating a self-standing air-clad PhC structure, which is the optimal one because of the larger  $k - \omega$  region available below the air light line. We believe that the proposed design concepts may be of importance for future research on photonic crystal-based optical circuits, not only for air-clad systems, but also for what concerns the use of large patterned areas on a single chip, in which robustness and integrability of a SOI structure would play a crucial role.

## Acknowledgments

The authors are grateful to M. Notomi for suggesting the investigation of the symmetrized SOI structure and for useful discussions. They are also indebted to M. Belotti and M. Galli for helpful suggestions on various experimental aspects. This work was supported by the Italian Ministry of University and Scientific Research (MIUR) through Cofin program “Silicon-based photonic crystals,” through FIRB project “Miniaturized electron and photon systems,” and by the National Institute for the Physics of Matter (INFM) through PRA PHOTONIC.